

# Cotreatment with 17-Allylamino-Demethoxygeldanamycin and FLT-3 Kinase Inhibitor PKC412 Is Highly Effective against Human Acute Myelogenous Leukemia Cells with Mutant FLT-3

Prince George,<sup>1</sup> Purva Bali,<sup>1</sup> Pamela Cohen,<sup>2</sup> Jianguo Tao,<sup>1</sup> Fei Guo,<sup>1</sup> Celia Sigua,<sup>1</sup> Anasuya Vishvanath,<sup>1</sup> Warren Fiskus,<sup>1</sup> Anna Scuto,<sup>1</sup> Srinivas Annavarapu,<sup>1</sup> Lynn Moscinski,<sup>1</sup> and Kapil Bhalla<sup>1</sup>

<sup>1</sup>Department of Interdisciplinary Oncology, Moffitt Cancer Center and Research Institute University of South Florida, Tampa, Florida, and <sup>2</sup>Novartis Pharmaceutical, Inc., East Hanover, New Jersey

## ABSTRACT

Presence of the activating length mutation (LM) in the juxtamembrane domain or point mutation in the kinase domain of FMS-like tyrosine kinase-3 (FLT-3) mediates ligand-independent progrowth and prosurvival signaling in approximately one-third of acute myelogenous leukemia (AML). PKC412, an inhibitor of FLT-3 kinase activity, is being clinically evaluated in AML. Present studies demonstrate that treatment of human acute leukemia MV4-11 cells (containing a FLT-3 LM) with the heat shock protein 90 inhibitor 17-allylamino-demethoxy geldanamycin (17-AAG) attenuated the levels of FLT-3 by inhibiting its chaperone association with heat shock protein 90, which induced the poly-ubiquitylation and proteasomal degradation of FLT-3. Treatment with 17-AAG induced cell cycle G<sub>1</sub> phase accumulation and apoptosis of MV4-11 cells. 17-AAG-mediated attenuation of FLT-3 and *p*-FLT-3 in MV4-11 cells was associated with decrease in the levels of *p*-AKT, *p*-ERK1/2, and *p*-STAT5, as well as attenuation of the DNA binding activity of STAT-5. Treatment with 17-AAG, downstream of STAT5, reduced the levels of c-Myc and oncostatin M, which are transactivated by STAT5. Cotreatment with 17-AAG and PKC412 markedly down-regulated the levels of FLT-3, *p*-FLT-3, *p*-AKT, *p*-ERK1/2, and *p*-STAT5, as well as induced more apoptosis of MV4-11 cells than either agent alone. Furthermore, the combination of 17-AAG and PKC412 exerted synergistic cytotoxic effects against MV4-11 cells. Importantly, 17-AAG and PKC412 induced more loss of cell viability of primary AML blasts containing FLT-3 LM, as compared with those that contained wild-type FLT-3. Collectively, these *in vitro* findings indicate that the combination of 17-AAG and PKC412 has high level of activity against AML cells with FLT-3 mutations.

## INTRODUCTION

FMS-like tyrosine kinase-3 (FLT-3) is a member of class III receptor tyrosine kinases, which is activated by FLT-3 ligand-dependent dimerization and autophosphorylation, resulting in progrowth and prosurvival signaling through STAT-5, Ras/Raf/ERK1/2, and PI3K/AKT pathways (1, 2). Activating length mutation (LM), *e.g.*, internal tandem duplication of the juxtamembrane domain, or the point mutation at the aspartate 835 within the tyrosine kinase domain of FLT-3 has been reported to occur in approximately one-third of patients with acute myelogenous leukemia (AML; Refs. 1, 2). These mutations lead to autophosphorylation and constitutive and ligand-independent activity of FLT-3 tyrosine kinase (1, 2). When transduced into primary murine bone marrow progenitor cells, mutant FLT-3 can induce a myeloproliferative disorder. In addition, FLT-3 mutation can transform and confer a leukemogenic potential in the mouse myeloid cells (3, 4). Several studies have indicated that the presence of FLT-3 LM or tyrosine kinase domain mutations confer poor prognosis in AML (1, 2, 5). On the basis of the success of imatinib against Bcr-Abl (6),

several inhibitors of FLT-3, including PKC412, have been developed and are being tested in patients with AML (7, 8). But unlike imatinib in chronic myelogenous leukemia, thus far, FLT-3 kinase inhibitors as single agents have yielded limited clinical success (2).

FLT-3 has been demonstrated to be a *bona fide* client protein for the chaperone heat shock protein (hsp) 90 (9). Treatment with hsp90 inhibitor, herbimycin A, radicicol, or 17-allylamino demethoxy geldanamycin (17-AAG) was shown to disrupt the chaperone association of FLT-3 with hsp90, directing FLT-3 to poly-ubiquitylation and proteasomal degradation (9, 10). A number of well-characterized, newly synthesized, or stress-denatured client proteins, including c-Raf, AKT, and FLT-3, require interaction with hsp90 to maintain a mature, stable, and functional conformation (11, 12). This is achieved by hsp90 through its ability to bind and release client proteins, which is driven by ATP binding and hydrolysis (11–13). ATP/ADP binding to a hydrophobic NH<sub>2</sub> terminus pocket alters hsp90 conformation resulting in its interaction with a cochaperone complex that protects or stabilizes the client proteins or with an alternative subset of cochaperones that directs the misfolded proteins to a covalent linkage with polyubiquitin and subsequent degradation by 26S proteasome (11–13). Benzoquinone ansamycin antibiotic geldanamycin and its less toxic analog 17-AAG directly bind to the ATP/ADP binding pocket, thereby replacing the nucleotide and inhibiting hsp90 function as a molecular chaperone for the client proteins (11–13). By blocking ATP binding to hsp90, 17-AAG stabilizes the hsp90 conformation that recruits hsp70-based cochaperone complex associated with the misfolded client proteins, which results in the ubiquitin-dependent proteasomal degradation of the client proteins (11–13). Because treatment with 17-AAG not only down-regulates FLT-3 but also the downstream progrowth and prosurvival signaling molecules, AKT and c-Raf (11–13), this raises the issue whether cotreatment with 17-AAG would augment the cytotoxic effects of the FLT-3 kinase inhibitor, PKC412. In the present studies, we demonstrate for the first time that treatment with the combination of 17-AAG and PKC412 exerts synergistic cytotoxic effects against cultured human leukemia cells containing FLT-3 LM. This is associated with marked attenuation of the levels of FLT-3 and *p*-FLT-3, as well as down-regulation of the levels of *p*-STAT5, *p*-AKT, *p*-ERK1/2, and transactivation by STAT5. Significantly, also, in primary AML cells that contain the activating LM or tyrosine kinase domain mutation in FLT-3, the combination of 17-AAG and PKC412 induced more apoptosis than either agent alone.

## MATERIALS AND METHODS

**Reagents.** 17-AAG was obtained from the Developmental Therapeutics Branch of CTEP/National Cancer Institute/NIH (Bethesda, MD). PKC412 was provided by Novartis Pharmaceuticals, Inc. (East Hanover, NJ). Antibodies for the immunoblot analyses were purchased as follows: FLT-3, STAT5, and c-Myc from Santa Cruz Biotechnology, Inc. (Santa Cruz, CA); *p*-FLT-3 and *p*-ERK1/2 from Cell Signaling Technology (Beverly, MA); *p*-STAT5 from Upstate Biotechnology, Inc. (Lake Placid, NY); and oncostatin M from R&D

Received 1/2/04; revised 2/23/04; accepted 3/17/04.

The costs of publication of this article were defrayed in part by the payment of page charges. This article must therefore be hereby marked *advertisement* in accordance with 18 U.S.C. Section 1734 solely to indicate this fact.

**Requests for reprints:** Kapil Bhalla, Moffitt Cancer Center & Research Institute, 12902 Magnolia Drive, MRC 3 East, Room 3056, Tampa, FL 33612. Phone: (813) 903-6861; Fax: (813) 903-6817; E-mail: bhalla@kbn@moffitt.usf.edu.

Systems, Inc. (Minneapolis, MN). Antibodies for the immunoprecipitation and/or immunoblot analyses of hsp70, hsp90, *p*-AKT, AKT, ERK1/2, and poly(ADP-ribose) polymerase were obtained, as described previously (14–16).

**Cell Culture.** Acute leukemia MV4-11 (containing a 30-bp long internal tandem duplication in the exon 14 of FLT-3) and RS4-11 (containing wild-type FLT-3) cells were obtained from American Tissue Culture Collection (Manassas, VA) and maintained in culture in RPMI medium containing 10% fetal bovine serum and passaged twice a week, as described previously (14–16). Logarithmically growing cells were exposed to the designated concentrations of 17-AAG and/or PKC412. After these treatments, cells were pelleted and washed free of the drug(s) before the performance of the studies described below. Primary leukemia blasts from four patients with AML in relapse were harvested and purified, as previously described (14), from the peripheral blood or bone marrow after informed consent as a part of a protocol study sanctioned by the local Institutional Review Board.

**Flow Cytometry for Cell Cycle Status.** The flow cytometric evaluation of the cell cycle status of cells was performed, as previously described (17, 18).

**Assessment of Percentage of Nonviable Cells.** Primary AML cells were stained with trypan blue (Sigma, St. Louis, MO). The numbers of nonviable cells were determined by counting the cells that showed trypan blue uptake in a hemocytometer and reported as percentage of untreated control cells.

**Apoptosis Assessment.** Untreated and drug-treated cells were stained with Annexin-V and propidium iodide, and the percentage of apoptotic cells were determined by flow cytometry, as described previously (16). Analysis of synergism between 17-AAG and PKC412 in inducing apoptosis of MV4-11 cells was performed by median dose effect analysis using the commercially available software (CalcuSyn, Biosoft, Ferguson, MO; Ref. 19).

**Morphology of Apoptotic Cells.** After drug treatment,  $50 \times 10^3$  cells were washed with PBS (pH 7.3) and resuspended in the same buffer. Cytospin preparations of the cell suspensions were fixed and stained with Wright stain. Cell morphology was determined by light microscopy. In all, five different fields were randomly selected for counting of at least 500 cells. The percentage of apoptotic cells was calculated for each experiment, as described previously (17, 18).

**Flow Cytometric Analysis of *p*-FLT-3 and FLT-3.** For surface FLT-3 expression, the cells were incubated with either 0.2  $\mu$ g of anti-FLT-3 antibody (sc-19635; Santa Cruz Biotechnology, Inc.) or concentration-matched isotype, control antibody (IgG1; Caltag, Burlingame, CA) diluted in the blocking buffer and kept on ice for 1 h. Cells are then washed twice in PBS (1 $\times$ ) and incubated for an additional 30 min on ice in the FITC-conjugated secondary antibody (Molecular Probes, Eugene, OR). To determine *p*-FLT-3 expression, leukemia cells were fixed in 1% formaldehyde and permeabilized by resuspending them for 30 min in ice-cold 90% methanol. After this, cells were washed twice in the blocking buffer [PBS (1 $\times$ ), containing 0.5% BSA] and then incubated for an additional 10 min at room temperature in the blocking buffer. Next, either 0.4  $\mu$ g of monoclonal antibody to *p*-FLT-3 or the isotype control antibody (IgG2b; Caltag) were added, and the cells incubated for 30 min, rinsed twice in the blocking buffer, followed by incubation with the FITC-conjugated secondary antibody (Molecular Probes). After 30 min of incubation, cells are washed twice with PBS (1 $\times$ ) and resuspended in 400  $\mu$ l PBS (1 $\times$ ). The fluorescence was analyzed by FACScan Cytometer (San Jose, CA).

**Western Analyses of Proteins.** Western analyses were performed using specific antisera or monoclonal antibodies according to previously reported protocols (17, 18). Horizontal scanning densitometry was performed on Western blots by using acquisition into Adobe Photoshop (Apple, Inc., Cupertino, CA) and analysis by the NIH Image Program. The expression of  $\beta$ -actin was used as a control for protein loading.

**Immunoprecipitation of FLT-3.** After the designated treatments, cells were lysed in the lysis buffer [20 mM Tris (pH 8), 150 mM sodium chloride, 1% NP40, 0.1 M sodium fluoride, 10% glycerol, 1 mM phenylmethylsulfonyl fluoride, 1 mM sodium orthovanadate, 2.5  $\mu$ g/ml leupeptin, and 5  $\mu$ g/ml aprotinin] for 30 min on ice and the nuclear and cellular debris cleared by centrifugation. Cell lysates (200  $\mu$ g) were incubated with the FLT-3-specific polyclonal antibody for 1 h at 4°C. To this, washed protein A-agarose beads were added and incubated overnight at 4°C for 2 h. The immunoprecipitates were washed three times in the lysis buffer, and proteins were eluted with the SDS sample loading buffer before the immunoblot analyses with specific antibodies against hsp90, hsp70, ubiquitin, or FLT-3 (14).

**Preparation of Detergent-Soluble and -Insoluble Fractions.** After the designated drug treatments, cells were lysed with TNSEV buffer [50 mM Tris-HCl (pH 7.5), 2 mM EDTA, 100 mM NaCl, 1 mM sodium orthovanadate, 1% NP40 containing 20  $\mu$ g/ml aprotinin, 20  $\mu$ g/ml leupeptin, 1 mM phenylmethylsulfonyl fluoride, 25 mM NAF, and 5 mM *N*-ethylmaleimide; Ref. 16]. The insoluble fraction (pellet) were solubilized with SDS buffer [80 mM Tris (pH 6.8), 2% SDS, 100 mM DTT, and 10% glycerol]. Fifty  $\mu$ g of proteins from the NP40-soluble and -insoluble fractions were separated on 7.5% SDS-polyacrylamide gel and analyzed by Western blotting (16).

**Electrophoretic Mobility Shift Assay for STAT5a.** Untreated or 17-AAG- and/or PKC412-treated cells were lysed, nuclear extracts were obtained, and the electrophoretic mobility shift assay for the DNA binding activity of STAT5a was performed, as described previously (15).

**Statistical Analysis.** Significant differences between values obtained in a population of leukemic cells treated with different experimental conditions were determined using the student *t* test. *P*s of <0.05 were assigned significance.

## RESULTS

**17-AAG Treatment Attenuates *p*FLT-3 and FLT-3 and Its Downstream Signaling through *p*-STAT5, *p*-AKT, and *p*-ERK1/2 in MV4-11 Cells.** On the basis of the recent studies that FLT-3 is a client protein chaperoned by hsp90, we first compared the effect of the hsp90 inhibitor 17-AAG on the levels of the hsp90 client proteins, including mutant FLT-3 and AKT. Additionally, we determined the effects of 17-AAG on the levels of *p*-STAT5, *p*-AKT, and *p*-ERK1/2 in MV4-11 versus RS4-11 cells. As previously shown in other leukemia cell types (16, 20), exposure to 0.1–1.0  $\mu$ M 17-AAG markedly induced hsp70 levels in a dose-dependent manner, both in MV4-11 and RS4-11 cells (Fig. 1A). Treatment with 0.25–1.0  $\mu$ M 17-AAG for 4 h markedly attenuated the mutant FLT-3 and *p*-FLT-3 levels in MV4-11 cells. In contrast, the exposure to 17-AAG did not decrease the wild-type FLT-3 levels in RS4-11 cells. Treatment with 17-AAG also attenuated *p*-STAT5 and *p*-AKT levels, more in MV4-11 than in RS4-11 cells (Fig. 1A). Longer exposure to 250 nM 17-AAG for intervals up to 24 h inhibited FLT-3, *p*-STAT5, and *p*-AKT more in MV4-11 than in RS4-11 cells (data not shown). Also, *p*-ERK1/2 levels considerably declined in MV4-11 cells after treatment with >500 nM 17-AAG (Fig. 1A). In contrast, untreated RS4-11 neither expressed *p*-FLT-3 nor *p*-ERK1/2 (Fig. 1A), but exposure to 500 nM 17-AAG down-modulated *p*-AKT in RS4-11 cells (Fig. 1A). Importantly, exposure to 250 nM 17-AAG for 4–16 h also inhibited the DNA binding activity of STAT5a more in MV4-11 (Fig. 1B) than RS4-11 cells (data not shown). In MV4-11 cells, this was associated with down-regulation of STAT5-transactivated c-Myc (Fig. 1A) and oncostatin M levels (data not shown; Ref. 21).

**PKC412 and 17-AAG Induce Cell Cycle G<sub>1</sub>-Phase Accumulation and Apoptosis of MV4-11 Cells.** Next, we determined the effect of 17-AAG or PKC412 on cell cycle status and apoptosis of MV4-11 versus RS4-11 cells. Data in the table in Fig. 2A show that treatment with 17-AAG for 24 h significantly increased, in a dose-dependent manner, the percentage of MV4-11 more than RS4-11 cells in the G<sub>1</sub> phase of the cell cycle. This was associated with concomitant decline in the percentages of 17-AAG-treated cells in the S and G<sub>2</sub>-M phases of the cell cycle, again, more in MV4-11 than RS4-11 cells. In addition, exposure to 0.1–1.0  $\mu$ M 17-AAG for 48 h induced, in a dose-dependent manner, more apoptosis of MV4-11 than RS4-11 cells (increase in the percentage of annexin V positive cells; *P* < 0.01; Fig. 2B). This was also associated with marked induction of poly(ADP-ribose) polymerase cleavage activity of the caspases in MV4-11 but not in RS4-11 cells (data not shown). These findings are similar to those observed after treatment of MV4-11 cells with the FLT-3 kinase inhibitor, PKC412. As shown in Fig. 3A, exposure of MV4-11 cells to

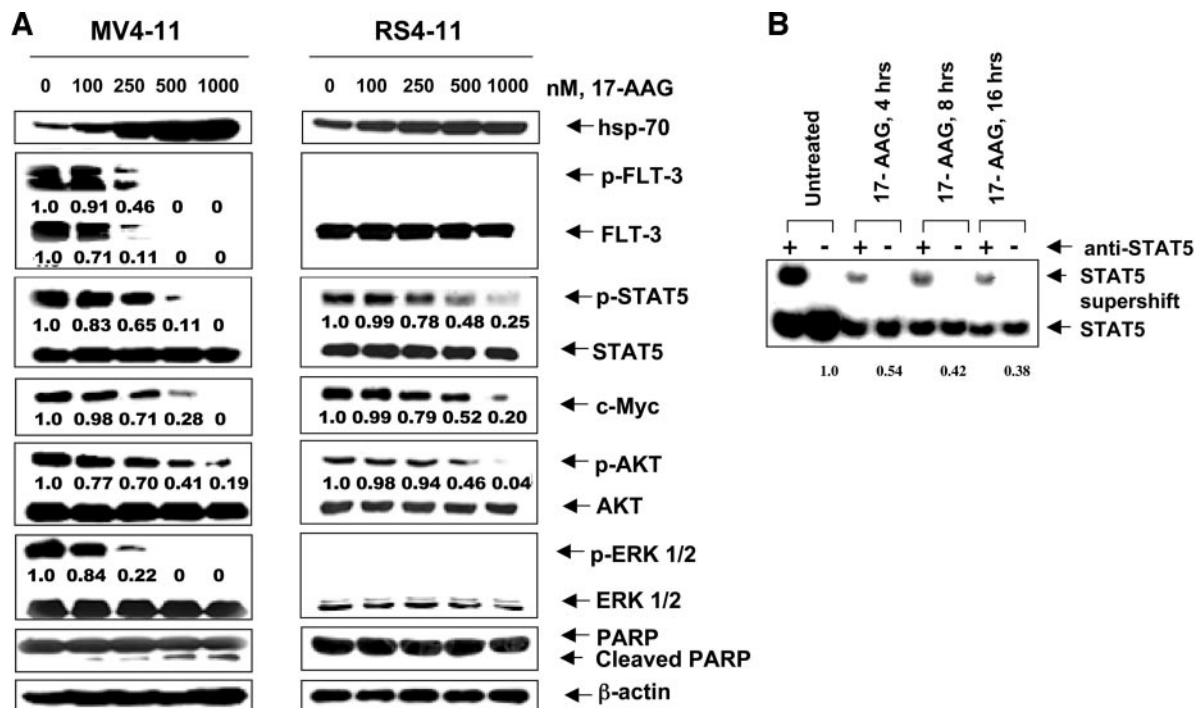


Fig. 1. 17-Allylamino-demethoxy geldanamycin (17-AAG) down-regulates *p*-FLT-3, mutant FLT-3, *p*-STAT5, *p*-AKT, and *p*-ERK1/2 and induces apoptosis of MV4-11 cells. **A**, Western blot analyses of heat shock protein 70 (hsp70), *p*-FLT-3, FLT-3, *p*-AKT, AKT, *p*-ERK1/2, ERK1/2, *p*-STAT5, STAT5, and poly(ADP-ribose) polymerase (PARP) in the cell lysates from MV4-11 and RS4-11 cells, after treatment with the indicated concentrations of 17-AAG for 4 h. The levels of β-actin served as the loading control. **B**, 17-AAG inhibits DNA binding activity of STAT5a. After treatment of MV4-11 cells with 250 nM 17-AAG for 4, 8, or 16 h, nuclear extracts were tested for the active STAT5a by electrophoretic mobility shift analysis. For supershift analysis, the nuclear extracts were treated with anti-STAT5 antibody before the addition of the poly(deoxyinosinic-deoxycytidylic acid) and the labeled DNA probe. Values underneath the bands represent the densitometric estimation of the density of the bands.

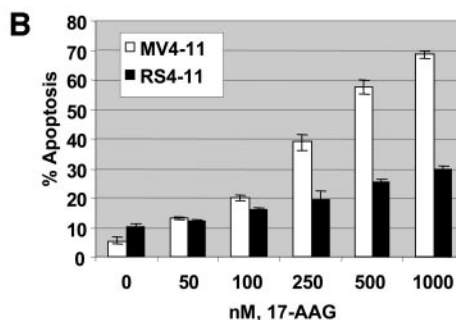
20 or 100 nM PKC412 induced significantly more apoptosis of MV4-11 than RS4-11 cells ( $P < 0.05$ ). Treatment with 100 nM PKC412 also resulted in attenuation of *p*-FLT-3, *p*-AKT, *p*-ERK1/2, and *p*-STAT5a levels in MV4-11 (Fig. 3B) but not in RS4-11 cells (data not shown). However, unlike 17-AAG, treatment with PKC412 only minimally attenuated the total intracellular levels or the cell-surface expression of FLT-3 (Figs. 3B and Fig. 4). We additionally compared the effects of 17-AAG and PKC412 on the surface expres-

sion of FLT-3 in the intact cells, as well as on the intracellular levels of *p*-FLT-3 in the permeabilized cells, using a novel flow cytometry based assay (see "Materials and Methods" above). Fig. 4 demonstrates that, although treatment with 100 nM 17-AAG for 24 h reduced both the surface expression of FLT-3 and the intracellular levels of *p*-FLT-3, PKC412 (50 nM for 24 h) only inhibited the levels of *p*-FLT-3 in MV4-11 cells. Higher concentrations of 17-AAG (500 nM) or of PKC412 (100 nM) inhibited the expression of FLT-3 and/or *p*-FLT-3,

**A** Effect of 17-AAG on Cell Cycle status of MV4-11 and RS4-11 cells

nM, 17-AAG	% of cells					
	MV4-11			RS4-11		
	G0/G1	S	G2/M	G0/G1	S	G2/M
0	52.6 ± 3.1	33.4 ± 1.1	13.9 ± 2.0	42.5 ± 0.5	44.2 ± 1.1	13.3 ± 0.7
50	65.0 ± 1.5	27.5 ± 1.8	7.4 ± 0.3	45.0 ± 1.4	46.4 ± 1.1	8.6 ± 1.5
100	74.1 ± 3.5	22.4 ± 2.1	3.3 ± 1.4	48.0 ± 1.5	43.9 ± 1.3	8.1 ± 1.4
250	83.6 ± 1.3	12.2 ± 2.3	2.0 ± 0.3	51.4 ± 2.8	40.8 ± 4.4	7.8 ± 1.5
500	86.3 ± 0.4	12.1 ± 1.1	1.4 ± 0.6	57.5 ± 4.9	34.1 ± 3.6	8.4 ± 1.8
1000	89.4 ± 4.0	9.9 ± 1.8	0.6 ± 2.2	75.7 ± 2.9	18.3 ± 3.1	6.0 ± 0.3

Fig. 2. 17-Allylamino-demethoxy geldanamycin (17-AAG) induces more cell cycle G<sub>1</sub>-phase accumulation and apoptosis in MV4-11 than RS4-11 cells. **A**, after treatment of MV4-11 or RS4-11 cells with the designated concentrations of 17-AAG, cell cycle status of the cells was determined by flow cytometry. **B**, MV4-11 and RS4-11 cells were treated with the indicated concentrations of 17-AAG for 48 h. After this, the percentage of annexin V-stained apoptotic cells was determined by flow cytometry.



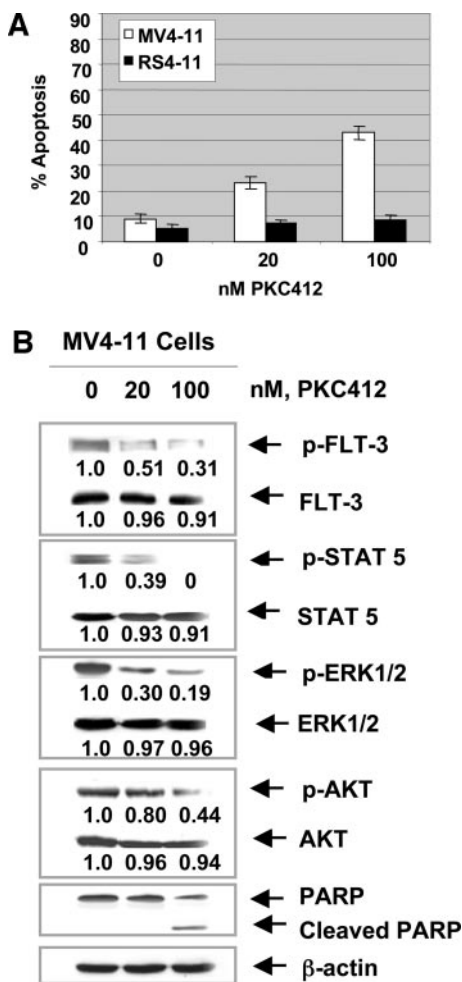


Fig. 3. PKC412 attenuates *p*-FLT-3, *p*-STAT5, *p*-AKT, and *p*-ERK1/2 and induces apoptosis of MV4-11 cells. **A**, MV4-11 and RS4-11 cells were treated with the indicated concentrations of PKC412 for 48 h. After this, the percentage of annexin V-stained apoptotic cells was determined by flow cytometry. **B**, after treatment with the indicated concentrations of PKC412 for 24 h, Western blot analyses of *p*-FLT-3, FLT-3, *p*-AKT, AKT, *p*-ERK1/2, ERK1/2, *p*-STAT5, STAT5, and poly(ADP-ribose) polymerase (PARP) was performed on the cell lysates from MV4-11 cells. The levels of  $\beta$ -actin served as the loading control. Values underneath the bands represent the densitometric estimation of the density of the bands.

respectively, to a greater extent (data not shown). Importantly, treatment with the combination of 17-AAG and PKC412 attenuated the expression *p*-FLT-3 significantly ( $P < 0.05$ ) more than treatment with either agent alone (Fig. 4). In contrast, after treatment with the combination of 17-AAG plus PKC412, the decline in FLT-3 expression was not significantly more than that observed after exposure to 17-AAG alone ( $P > 0.05$ ). Although the mechanism underlying this is unclear, the combination of 17-AAG and PKC412 also lowered the expression of FLT-3 more than treatment with 17-AAG alone (Fig. 4). Data presented in Fig. 4 are representative of three experiments.

#### 17-AAG Inhibits Chaperone Association of hsp90 with FLT-3, Promoting Its Poly-Ubiquitylation and Proteasomal Degradation.

We next determined the effect of 17-AAG on the chaperone association of FLT-3 with hsp90. As shown in Fig. 5A, treatment with 100 or 250 nM 17-AAG for 4 or 8 h significantly disrupted the chaperone association of FLT-3 with hsp90, thereby shifting the binding of FLT-3 from hsp-90 to a cochaperone complex that included hsp70 (11, 12). Consistent with this, as has been demonstrated for the other client proteins of hsp-90, *e.g.*, Bcr-Abl and c-Raf, treatment with 17-AAG directed FLT-3 to poly-ubiquitylation, which is shown in Fig. 5B as increased poly-ubiquitylation of proteins in the immunoprecipitates of FLT-3. Treatment of MV4-11 cells with the proteasome inhibitor ALLnL, which blocked their proteasomal degradation, also increased the amount of poly-ubiquitylated proteins (Fig. 5B). In addition, as compared with either treatment alone, cotreatment with 17-AAG and ALLnL increased accumulation of the poly-ubiquitylated proteins in the immunoprecipitates of FLT-3 (Fig. 5B). After treatment with 17-AAG, the disruption of the chaperone association between FLT-3 and hsp90 also resulted in the significant increase of FLT-3 in the detergent (NP40)-insoluble fraction, with concomitant significant decline in the detergent-soluble fraction of MV4-11 cells. This would lead to the degradation of poly-ubiquitylated FLT-3 by the 26S proteasome (Fig. 5, B and C). Cotreatment with ALLnL, while increasing the accumulation of FLT-3 in the detergent-insoluble fraction, restored 17-AAG-mediated decline in the detergent-soluble fraction of MV4-11 cells (Fig. 5C).

#### Cotreatment with 17-AAG and PKC412 Exerts Synergistic Cytotoxic Effects and Markedly Attenuates STAT5 DNA Binding Activity in MV4-11 Cells.

We next determined the apoptotic effects of 17-AAG and PKC412 in MV4-11 cells. Fig. 6A shows that as compared with treatment with 50 or 100 nM 17-AAG or 20, 50, or 100

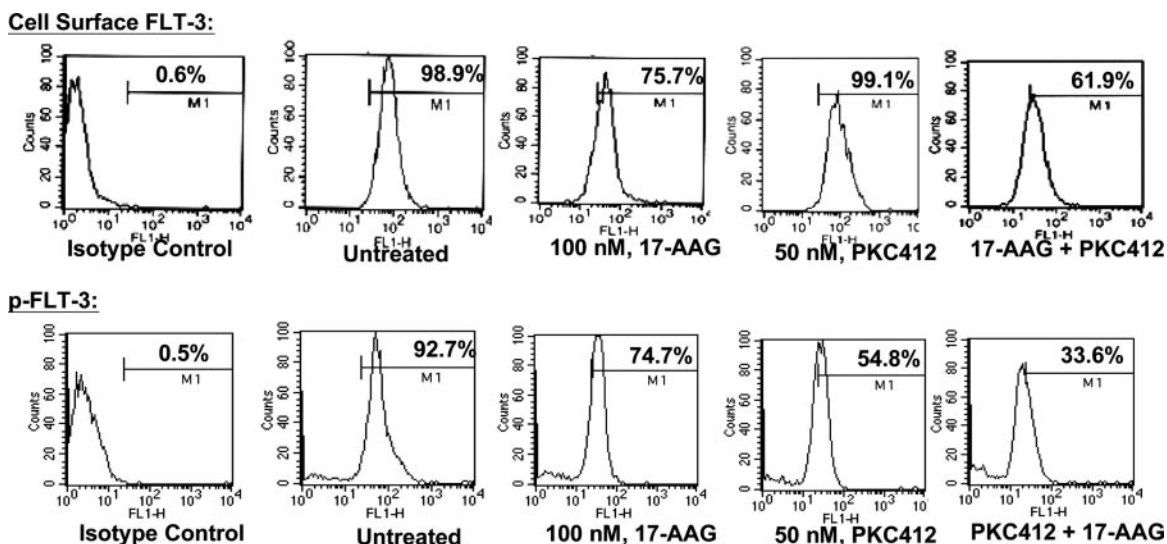
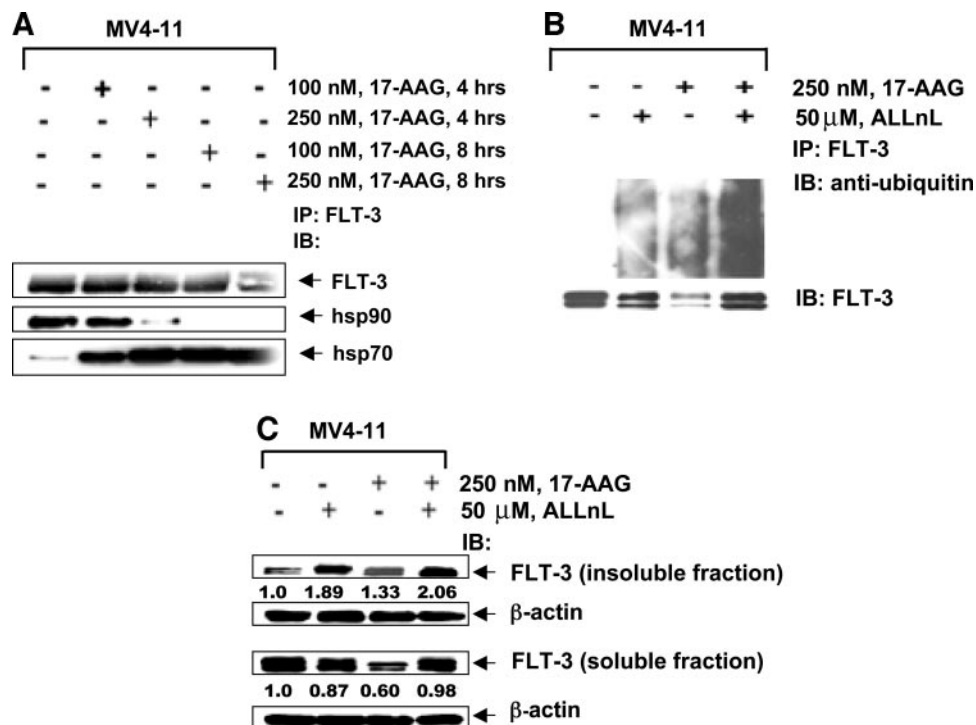


Fig. 4. MV4-11 cells were exposed to the indicated concentrations of 17-AAG and/or PKC412 for 24 h. After this, the cell surface expression of FLT-3 in intact cells or the intracellular levels of *p*-FLT-3 cells in the permeabilized cells was determined by flow cytometry. The histograms in the panels are representative of three experiments. Values in each panel represent the percentage of cells showing positive staining.

Fig. 5. 17-Allylamino-demethoxy geldanamycin (17AAG) inhibits the chaperone association of FLT-3 with heat shock protein (hsp) 90 and promotes the poly-ubiquitylation and proteasomal degradation of FLT-3. A, MV4-11 cells were treated with the indicated concentration of 17-AAG for 4 or 8 h. After this, immunoprecipitates of FLT-3 from the cell lysates were immunoblotted with anti-hsp90, anti-hsp70, or anti-FLT-3 antibodies. B, MV4-11 cells were treated with the indicated concentrations of 17-AAG and/or ALLnL or either agent alone for 8 h. After this, the immunoprecipitates of FLT-3 from the cell lysates were immunoblotted with anti-ubiquitin or anti-FLT-3 antibody. C, MV4-11 cells were either cotreated with the indicated concentrations of 17-AAG and ALLnL or either agent alone for 4 h. The detergent (NP40)-soluble or -insoluble fractions were immunoblotted with anti-FLT-3 antibody. The levels of  $\beta$ -actin served as the loading control. Values underneath the bands represent the densitometric estimation of the density of the bands.

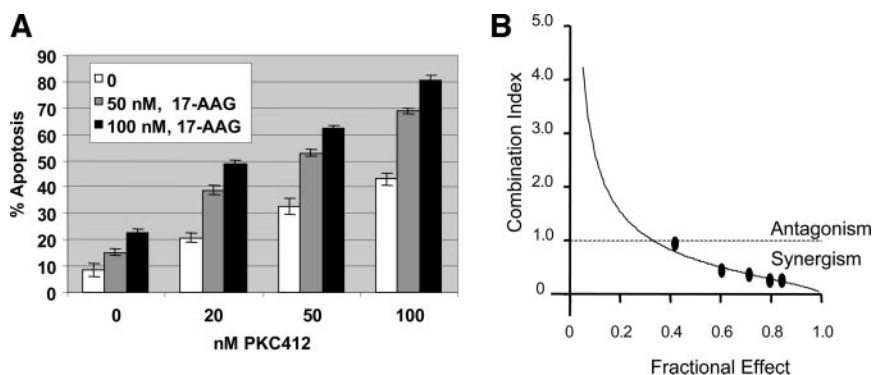


nM PKC412 alone for 48 h, the combined treatment with 17-AAG and PKC412 induced more apoptosis of MV4-11 cells. Additionally, cotreatment with 100 nM PKC412 and 100 nM 17-AAG for a shorter interval of 24 h induced more apoptosis than treatment with either agent alone (percentage of apoptosis in untreated control cells:  $5.2 \pm 0.8$ ; treated with 17-AAG:  $13.2 \pm 1.4$ ; PKC412:  $27.9 \pm 2.5$ ; and 17-AAG plus PKC412:  $41.8 \pm 2.2$ ). The combination also induced more poly(ADP-ribose) polymerase cleavage activity of the effector caspases associated with apoptosis (Fig. 7A). Importantly, exposure to the combination of 17-AAG and PKC412 exerted synergistic apoptotic effect in MV4-11 cells, as determined by the median dose effect analysis, which revealed combination index values of  $<1.0$  (Fig. 6B). As compared with either agent alone, cotreatment with 17-AAG (100 nM) and PKC412 (50 nM) was associated with more decline in the expression of *p*-FLT-3, *p*-STAT5, *p*-AKT, and *p*-ERK1/2 in MV4-11 cells (Fig. 7A). As compared with the untreated MV4-11 cells, treatment with 100 nM 17-AAG and 50 nM PKC412 attenuated the DNA binding of STAT5a by  $\sim 27$  and 80% (relative density of 1.0 *versus* 0.73 and 0.20 by densitometry of the bands; Fig. 7B). Combined treatment with 17-AAG and PKC412 almost completely inhibited the DNA binding activity of STAT5a (Fig. 7B). These results are representative of two separate experiments and are

consistent with the greater decline in the *p*-FLT-3 and *p*-STAT5 levels due to treatment with the combination (Fig. 7A). The decline in STAT5 activity was also associated with greater attenuation of the levels of c-Myc and oncostatin M (Fig. 7A).

**Cotreatment with 17-AAG and PKC412 Causes More Attenuation of *p*-FLT-3 and Apoptosis of Primary AML Cells with FLT-3 Mutation Than either Agent Alone.** We next determined whether the combination of 17-AAG and PKC412 *versus* either agent alone would also have superior activity against primary AML cells isolated from the peripheral blood and/or bone marrow samples from four patients with AML in relapse. Although not shown, sample no. 1 cells contained a duplication of a 51-bp sequence (from bp 1837 to 1887) and sample no. 2 cells contained a point mutation D835Y in FLT-3. Samples nos. 3 and 4 contained the wild-type FLT-3 (data not shown). The table in Fig. 8A indicates that in sample nos. 1 and 2, cotreatment for 48 h with 17-AAG (250 nM) and PKC412 (100 or 500 nM) resulted in a markedly higher percentage of nonviable cells than treatment with either agent alone (values represent mean of two experiments performed in duplicate). In contrast, this was not the case in sample nos. 3 and 4. Although exposure to 17-AAG slightly increased the percentage of nonviable cells in a dose-dependent manner in sample nos. 3 and 4, this was clearly less than in sample nos.

Fig. 6. Cotreatment with 17-allylamino-demethoxy geldanamycin (17-AAG) and PKC412 induces more apoptosis and exerts synergistic cytotoxic effects in MV4-11 cells. A, MV4-11 cells were treated with the indicated concentrations of 17-AAG and/or PKC412 for 48 h. After this, the percentage of annexin V-stained apoptotic cells was determined by flow cytometry. B, using CalcuSyn software (Biosoft), the analysis of the dose-effect relationship for 17-AAG and/or PKC412-induced loss of viability was performed according to the median effect method of Chou and Talalay, and the combination index (CI) values were calculated for three independent experiments.  $CI < 1$ ,  $CI = 1$ , and  $CI > 1$  represent synergism, additivity, and antagonism of the two agents, respectively.



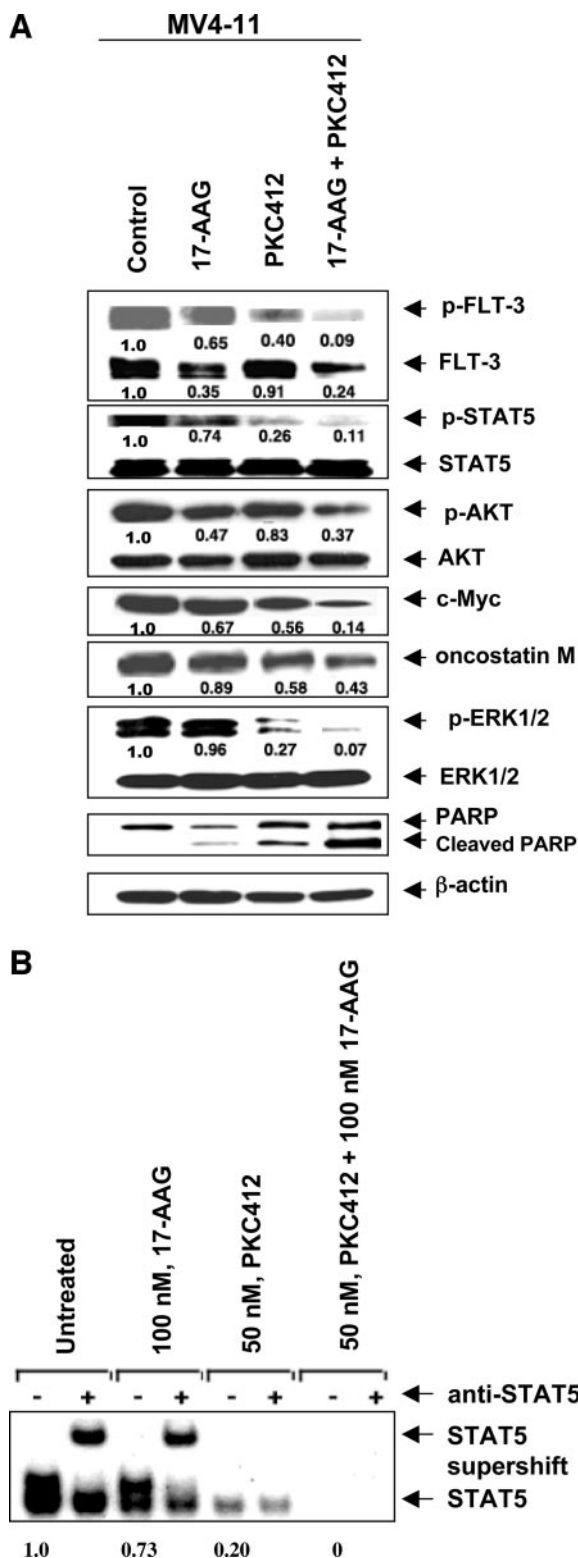


Fig. 7. Cotreatment with 17-allylamino-demethoxy geldanamycin (17-AAG) and PKC412 attenuates *p*-FLT-3, *p*-STAT5, *p*-AKT, and *p*-ERK1/2, as well as inhibits STAT5a DNA binding activity, more than either agent alone. **A**, after treatment with 100 nM 17-AAG and/or 50 nM PKC412 for 24 h, Western blot analyses of *p*-FLT-3, FLT-3, *p*-AKT, AKT, *p*-ERK1/2, ERK1/2, *p*-STAT5, STAT5, c-Myc, oncostatin M, and poly(ADP-ribose) polymerase (PARP) were performed in the cell lysates from MV4-11 cells. The levels of  $\beta$ -actin served as the loading control. **B**, after treatment of MV4-11 cells with 100 nM 17-AAG and/or PKC412 for 24 h, nuclear extracts were tested for the active STAT5a by electrophoretic mobility shift analysis. For supershift analysis, the nuclear extracts were treated with anti-STAT5 antibody before the addition of the poly(deoxyinosinic-deoxycytidylic acid) and the labeled DNA probe. Values underneath the bands represent the densitometric estimation of the density of the bands.

1 and 2. PKC412 treatment also increased the percentage of nonviable cells in sample nos. 1 and 2 in a dose-dependent manner, whereas there was a minimal increase in the percentage of nonviable cells in sample nos. 3 and 4. After treatment with 17-AAG, Western blot analyses of the total cell lysates of sample no. 1 showed a dose-dependent 17-AAG-mediated attenuation of the levels of the FLT-3, *p*-FLT-3, *p*-STAT5, *p*-AKT, and AKT levels, without significant alteration in STAT5 and *p*-ERK1/2 and ERK1/2 (data not shown). 17-AAG induced hsp70 levels in the primary leukemia cells (Fig. 8B). Additionally, after cotreatment with 17-AAG and PKC412, Western blot analyses of the total cell lysates of sample no. 1 showed a greater decline in the *p*-FLT-3 and FLT-3 levels than treatment with either agent alone (Fig. 8C). These data corroborate the results of the studies in the cultured leukemia cells.

## DISCUSSION

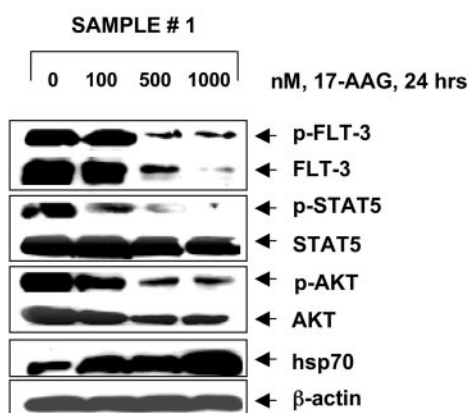
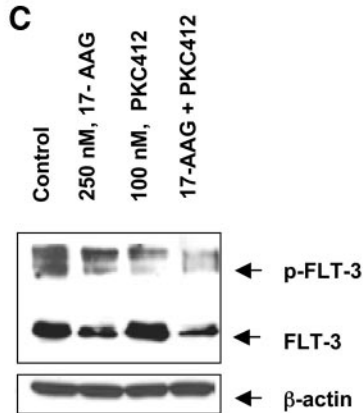
MV4-11 cells contain an internal tandem duplication of a 30-bp long internal tandem duplication in the exon 14 of FLT-3, which is representative of the activating mutations that result in autophosphorylation of FLT-3 in AML (10). Present studies clearly demonstrate that exposure to 17-AAG, in a dose-dependent manner, reduces the levels of *p*-FLT-3 and FLT-3 in MV4-11 more than the levels of the wild-type FLT-3 in RS4-11 cells. 17-AAG-mediated attenuation of the *p*-FLT-3 was most likely caused by inhibition of its autophosphorylation, although it could also be caused by 17-AAG-induced activity of a phosphatase involved in dephosphorylation of FLT-3. Previous studies have shown that the autophosphorylation and binding of the cytosolic domain of FLT-3 to the p85 subunit of PI3K, GRB2, SRC and SHC results in the activation of Ras-Raf-ERK1/2, PI3K-AKT, and STAT5 signaling pathways, which promote cell growth and survival (1, 2, 22). In addition, presence of mutant FLT-3 has been significantly correlated with constitutive activation of STAT5 (1, 2, 23). The importance of STAT5a in this signaling is highlighted by the observations that FLT-3 ligand is able to induce proliferation of STAT5a  $+/+$  or STAT5b  $-/-$  but not of STAT5a  $-/-$  hematopoietic progenitor cells (24). Present studies also clearly demonstrate that treatment with 17-AAG results in greater attenuation of *p*-STAT5, *p*-AKT, and *p*-ERK1/2 levels in MV4-11 than RS4-11 cells. 17-AAG also inhibited STAT5 DNA binding in MV4-11 cells. Recently, FLT-3-STAT5 pathway was shown to be a potential target for therapy in AML with mutations in FLT-3 (23). Because treatment with 17-AAG attenuated *p*-STAT5, *p*-AKT, and *p*-ERK1/2 levels in primary AML cells with mutant FLT-3, 17-AAG promises to be an effective component of novel therapy of AML.

Importantly, as compared with either agent alone, co-treatment with 17-AAG and PKC412 produced more decline in *p*-STAT5, *p*-AKT, and *p*-ERK1/2 levels in MV4-11 cells. Additionally, cotreatment with 17-AAG and PKC412 also inhibited DNA binding of STAT5. A marked decline in the genes downstream of STAT5a that promote cell proliferation and survival, *e.g.*, c-Myc, Pim-2, and oncostatin M, coupled with the decline in the levels of *p*-AKT and *p*-ERK1/2 may be responsible for the synergistic apoptotic effects observed after treatment with the combination of 17-AAG and PKC412 (20, 21). Recently, FLT-3 mutations have also been discovered in patients with acute lymphoblastic leukemia with mixed lineage leukemia (MLL) rearrangements, and PKC412 was also shown to have activity against this type of acute lymphoblastic leukemia (25). This suggests that the combination of 17-AAG and PKC412 may also have efficacy against acute lymphoblastic leukemia with MLL rearrangements. Recently, it was shown that diverse mutations in FLT-3 could have different sensitivity to the various FLT-3 kinase inhibitors currently being evaluated against AML (26). In light of this, cotreatment with 17-

**A**

Patient #	% Cell Death						
	Control	nM, PKC412		nM, 17-AAG		250 nM, 17-AAG plus nM, PKC412	
		100	500	250	1000	100	500
1	12.9	27.1	64.9	44.6	64.0	64.6	73.8
2	11.1	23.3	41.1	33.0	53.8	51.7	69.7
3	10.2	15.8	19.8	19.4	24.0	16.9	25.9
4	10.0	9.9	10.1	15.8	16.5	13.0	16.6

Fig. 8. Cotreatment with 17-allylamino-demethoxy geldanamycin (17-AAG) and PKC412 induces more loss of cell viability than either agent alone in primary acute myelogenous leukemia cells with mutant FLT-3. **A**, primary acute myelogenous leukemia cells with FLT-3 internal tandem duplication (sample no. 1) or tyrosine kinase domain mutation (sample no. 2) or wild-type FLT-3 (sample nos. 3 and 4) were treated with the indicated concentrations of 17-AAG and/or PKC412 for 48 h, and the percentage of nonviable cells were determined. The values represent mean of two experiments performed in duplicate. **B**, after treatment with the indicated concentrations of 17-AAG for 24 h, Western blot analyses of *p*-FLT-3, FLT-3, *p*-AKT, AKT, *p*-STAT5, STAT5, and heat shock protein 70 (hsp70) in the lysates from sample no. 1 cells. The levels of  $\beta$ -actin served as the loading control. **C**, Western blot analyses of *p*-FLT-3 and FLT-3 in the cell lysates from the cells in sample no. 1, after treatment with 250 nM 17-AAG and/or 100 nM PKC412 for 24 h.

**B****C**

AAG and PKC412 may potentially be more effective than treatment with a FLT-3 tyrosine kinase inhibitor alone against AML or acute lymphoblastic leukemia with FLT-3 mutations. Individually, 17-AAG and PKC412 also appear to be relatively more toxic to leukemia than normal bone marrow progenitor cells and thus far have not exhibited *in vivo* dose-limiting toxicity in the bone marrow (1, 27, 28). However, the *in vitro* and *in vivo* cytotoxic effects of 17-AAG and PKC412 against normal human bone marrow progenitor cells remain to be fully evaluated.

Similar to FLT-3, Bcr-Abl tyrosine kinase is a client protein for hsp90, and it is noteworthy that 17-AAG-mediated inhibition of hsp90 promotes proteasomal degradation and attenuation of the mutant form of Bcr-abl, which is resistant to imatinib more than the wild-type Bcr-Abl (15, 16, 29). In the present studies, a similar increased sensitivity to 17-AAG-mediated attenuation of FLT-3 LM was observed in MV4-11, as compared with the wild-type FLT-3 in RS4-11 cells. This may be because the mutant FLT-3 (also mutant Bcr-Abl) is more dependent on hsp90 for retaining a mature, stable, and functional conformation than the wild-type FLT-3. This would explain why 17-AAG-mediated inhibition of hsp90 could direct FLT-3 LM to poly-ubiquitylation and proteasomal degradation to a greater extent than wild-type FLT-3. Furthermore, it is also possible that AML cells that contain FLT-3 LM are more dependent on its progrowth and prosurvival signaling. This could be responsible for the synergistic apoptotic effects observed following marked attenuation of *p*-FLT-3 and its downstream signaling due to treatment of MV4-11 cells with 17-AAG and PKC412. It is noteworthy that PKC412 is also known to inhibit the isoforms  $\alpha$ ,  $\beta$ , and  $\gamma$  of protein kinase C (30). Consistent with this 17-AAG has also been shown to synergize with UCN-01 against leukemia cells (31).

A flow cytometry-based assay described here was used to measure

the effect of 17-AAG and/or PKC412 on the expression of the surface FLT-3, as well as on the *p*-FLT-3 levels. Although treatment with 17-AAG reduced both the surface expression of FLT-3 and the intracellular levels of *p*-FLT-3, PKC412 treatment only inhibited the levels of *p*-FLT-3 in MV4-11 cells. Importantly, treatment with the combination of 17-AAG and PKC412 attenuated the expression *p*-FLT-3 more than treatment with either agent alone. Although the mechanism underlying this is unclear, the combination of 17-AAG and PKC412 also lowered the expression of FLT-3 more than treatment with 17-AAG alone. Although promising, the specificity and reliability of the flow cytometry assay as a surrogate for FLT-3 gene sequencing in primary AML cells remains to be established. If validated, this relatively simple, easy, and inexpensive assay could replace the currently used more labor-intensive molecular sequencing assay for diagnosing the presence of the FLT-3 mutations and serving as a biomarker for the efficacy of anti-FLT-3 strategies in human acute leukemia.

In summary, the data presented here strongly suggest that as compared with either agent alone, the combination of 17-AAG and PKC412 exerts greater cytotoxicity against AML cells with FLT-3 mutations. Because treatment with 17-AAG is known to lower a number of signaling molecules in addition to and downstream of FLT-3 (10, 11), the inclusion of 17-AAG in this anti-AML regimen may especially enhance its activity against AML cells with constitutively active growth and survival signaling pathways (1, 2). Collectively, these findings generate a strong rationale to investigate the clinical efficacy of the combination of 17-AAG and PKC412 against a variety of hematological malignancies in relapse where the leukemia cells harbor activating LM or tyrosine kinase domain mutations and constitutive activation of FLT-3.

## REFERENCES

- Gilliland DG, Griffin JD. The roles of FLT3 in hematopoiesis and leukemia. *Blood* 2002;100:1532–42.
- Stirewalt DL, Radich J. The role of FLT3 in haematopoietic malignancies. *Nat Rev Cancer* 2003;3:650–65.
- Kelly LM, Liu Q, Kutok JL, Williams IR, Boulton CL, Gilliland DG. FLT3 internal tandem duplication mutations associated with human acute myeloid leukemias induce myeloproliferative disease in a murine bone marrow transplant model. *Blood* 2002;99:310–8.
- Tse K-F, Mukherjee G, Small D. Constitutive activation of FLT3 stimulates multiple intracellular signal transducers and results in transformation. *Leukemia (Baltimore)* 2000;14:1766–76.
- Schnittger S, Schoch C, Dugas M, et al. Analysis of FLT3 length mutations in 1003 patients with acute myeloid leukemia: correlation to cytogenetics, FAB subtype, and prognosis in the AMLCG study and usefulness as a marker for the detection of minimal residual disease. *Blood* 2002;100:59–66.
- Savage DG, Antman KH. Imatinib mesylate: a new oral targeted therapy. *N Engl J Med* 2002;28:689–93.
- Weisberg E, Boulton C, Kelly LM, et al. Inhibition of mutant FLT3 receptors in leukemia cells by the small molecule tyrosine kinase inhibitor PKC412. *Cancer Cell* 2002;1:433–43.
- Sawyers CL. Finding the next Gleevec: FLT3 targeted kinase inhibitor therapy for acute myeloid leukemia. *Cancer Cell* 2002;1:413–5.
- Minami Y, Kiyoi H, Yamamoto Y, et al. Selective apoptosis of tandemly duplicated FLT3-transformed leukemia cells by Hsp90 inhibitors. *Leukemia (Baltimore)* 2002;16:1535–40.
- Yao Q, Nishiuchi R, Li Q, Kumar AR, Hudson WA, Kersey JH. FLT3 expressing leukemias are selectively sensitive to inhibitors of the molecular chaperone heat shock protein 90 through destabilization of signal transduction-associated kinases. *Clin Cancer Res* 2003;9:4483–93.
- Blagosklonny MV. Hsp-90-associated oncoproteins: multiple targets of geldanamycin and its analogs. *Leukemia (Baltimore)* 2002;16:455–62.
- Isaacs HS, Xu W, Neckers L. Heat shock protein 90 as a molecular target for cancer therapeutics. *Cancer Cell* 2003;3:213–7.
- Grenert JP, Sullivan WP, Fadden P, et al. The amino-terminal domain of heat shock protein 90 (hsp90) that binds geldanamycin is an ATP/ADP switch domain that regulates hsp90 conformation. *J Biol Chem* 1997;272:23843–50.
- Nimmanapalli R, Fuino L, Bali P, et al. Histone deacetylase inhibitor LAQ824 both lowers expression and promotes proteasomal degradation of Bcr-Abl and induces apoptosis of Imatinib Mesylate-sensitive or -refractory chronic myelogenous leukemia-blast crisis cells. *Cancer Res* 2003;63:5126–35.
- Nimmanapalli R, O'Bryan E, Huang M, et al. Molecular characterization and sensitivity of STI-571 (Imatinib Mesylate, Gleevec)-resistant, Bcr-Abl positive, human acute leukemia cells retain sensitivity to SRC kinase inhibitor PD180970 and 17-allylamino-17-demethoxygeldanamycin (17-AAG). *Cancer Res* 2002;62:5761–9.
- Nimmanapalli R, O'Bryan E, Bhalla K. Geldanamycin and its analogue 17-allylamino-17-demethoxygeldanamycin lowers Bcr-Abl levels and induces apoptosis and differentiation of Bcr-Abl-positive human leukemic blasts. *Cancer Res* 2001;61:1799–804.
- Fang G, Kim C, Perkins C, et al. CGP57148 (STI-571) induces differentiation and apoptosis and sensitizes Bcr-Abl positive human leukemia cells to apoptosis due to antileukemic drugs. *Blood* 2000;96:2246–56.
- Ibrado AM, Huang Y, Fang G, Bhalla K. Bcl-x<sub>L</sub> overexpression inhibits Taxol-induced Yama protease activity and apoptosis. *Cell Growth Differ* 1996;7:1087–94.
- Chou TC, Talalay P. Quantitative analysis of dose-effect relationships: the combined effects of multiple drugs or enzyme inhibitors. *Adv Enzyme Regul* 1984;22:27–55.
- Nimmanapalli R, O'Bryan E, Kuhn D, Yamaguchi H, Wang H-G, Bhalla K. Regulation of 17-AAG-induced apoptosis: role of Bcl-2, Bcl-x<sub>L</sub>, and Bax downstream of 17-AAG-mediated down-regulation of Akt, Raf-1, and Src kinases. *Blood* 2003;102:269–75.
- Mizuki M, Schwäbe J, Steur C, et al. Suppression of myeloid transcription factors and induction of STAT response genes by AML-specific Flt3 mutations. *Blood* 2003;101:3164–73.
- Dosil M, Wang S, Lemischka IR. Mitogenic signaling and substrate specificity of the Flk2/Flt3 receptor tyrosine kinase in fibroblasts and interleukin 3-dependent hematopoietic cells. *Mol Cell Biol* 1993;13:6572–85.
- Spiekermann K, Bagrintseva K, Schwab R, Schmieja K, Hiddemann W. Overexpression and constitutive activation of FLT3 induces STAT5 activation in primary acute myeloid leukemia blast cells. *Clin Cancer Res* 2003;9:2140–50.
- Zhang S, Fukuda S, Lee Y, et al. Essential role of signal transducer and activator of transcription (Stat)5a but not Stat5b for Flt3-dependent signaling. *J Exp Med* 2000;192:719–28.
- Armstrong SA, Kung AL, Mabon ME, et al. Inhibition of FLT3 in MLL: validation of a therapeutic target identified by gene expression based classification. *Cancer Cell* 2003;3:173–83.
- Grundler R, Thiede C, Miething C, Steudel C, Peschel C, Duyster J. Sensitivity toward tyrosine kinase inhibitors varies between different activating mutations of the FLT3 receptor. *Blood* 2003;102:646–51.
- Estey EH, Fisher T, Giles F, et al. A randomized Phase II trial of the tyrosine kinase inhibitor PKC412 in patients (pt) with acute myeloid leukemia (AML)/high-risk myelodysplastic syndromes (MDS) characterized by wild-type (WT) or mutated FLT3 [abstract]. *Blood* 2003;102:2270.
- Solit DB, Anana M, Valentin G, et al. Phase I trial of 17-AAG (17-allylamino-17-demethoxygeldanamycin) in patients (pt) with advanced cancer [abstract]. *Proc Am Soc Clin Oncol* 2003;22:795.
- Gorre ME, Ellwood-Yen K, Chiosis G, Rosen N, Sawyers CL. BCR-ABL point mutants isolated from patients with imatinib mesylate-resistant chronic myeloid leukemia remain sensitive to inhibitors of the BCR-ABL chaperone heat shock protein 90. *Blood* 2002;100:3041–4.
- Nakamura K, Yoshikawa N, Yamaguchi Y, Kagota S, Shinozuka K, Kunitomo M. Effect of PKC412, an inhibitor of protein kinase C, on spontaneous metastatic model mice. *Anticancer Res* 2003;23:1395–9.
- Jia W, Yu C, Rahmani M, et al. Synergistic antileukemic interactions between 17-AAG and UCN-01 involve interruption of RAF/MEK- and AKT-related pathways. *Blood* 2003;102:1824–32.